Pharmacological basis for application of scutellarin in Alzheimer's disease: Antioxidation and antiapoptosis

XINYU HU[1], SHANSHAN TENG[2], JIAWEI HE[2,3], XIAOQI SUN[1],
MINGZHAO DU[2,4], LING KOU[2,4] and XIAOFENG WANG[2,5]

[1]Faculty of Clinical Medicine, Changchun Medical College, Changchun, Jilin 130031;
[2]School of Life Sciences, Jilin University, Changchun, Jilin 130012; [3]Department of Pharmacy and Food Science,
Zhuhai College of Jilin University, Jilin University, Zhuhai, Guangdong 519000; [4]Department of Cardiology,
Affiliated Hospital of Jiangsu University, Jiangsu University, Zhenjiang, Jiangsu 212001; [5]Department of Stomatology,
China-Japan Union Hospital of Jilin University, Jilin University, Changchun, Jilin 130033, P.R. China

Abstract. Scutellarin (SC), mainly extracted from the Chinese herb *Erigeron breviscapus* (vant.), has been reported to possess various pharmacological activities; however, its effects on Alzheimer's disease (AD) have not been systemically reported. The protective effects of SC on AD were investigated using an L-glutamic acid (L-Glu)-damaged HT22 cell apoptosis model and an aluminum chloride plus D-galactose-induced AD mouse model. In L-Glu-damaged HT22 cells, SC significantly increased cell viability, inhibited lactate dehydrogenase release, reduced caspase-3 activity and suppressed apoptosis, which were determined via an MTT assay, an *in vitro* Toxicology Assay kit, a Caspase-3 activity assay kit, and propidium iodide and Annexin V staining. Furthermore, SC suppressed the accumulation of intracellular reactive oxygen species (ROS), restored the dissipation of mitochondrial membrane potential, enhanced the expression of antiapoptotic proteins and reduced the expression of pro-apoptotic proteins, as determined by immunofluorescence assays and western blotting. In AD mice, SC enhanced vertical and horizontal movements in an autonomic activity test, and reduced the escape latency time in the water maze test. SC reduced the deposition of amyloid β1-42 (Aβ1-42) and the expression of phosphorylated-Tau in the hippocampus as determined by immunohistochemistry analysis, but enhanced the serum levels of Aβ1-42 of AD mice as determined by ELISA. ELISA analyses also revealed that SC enhanced the levels of acetylcholine, and superoxide dismutase in serum and brain lysate, whereas reduced the levels of ROS in brain lysate of AD mice. The present study confirmed that the protective effects of SC in AD *in vitro* and *in vivo* are associated with its antioxidant and antiapoptotic properties.

Introduction

Alzheimer's disease (AD), which is caused by the loss of neurons and synapse degeneration, is clinically characterized by changes in cognitive function (1), which affects >47 million people worldwide (2). Due to its complex pathological mechanism, its therapeutic targets have not yet been identified (3). A widely accepted hypothesis is that oxidative stress serves an important role in the progression of AD as amyloid β (Aβ) aggregation has been observed and often accompanied with neurotoxic reactive oxygen species (ROS) production (4). Glutamate, a neurotransmitter in the central nervous system, contributes to this process by causing the accumulation intracellular ROS (5). ROS overproduction and Aβ aggregation are not only responsible for synaptic dysfunction, but also cause mitochondria-mediated apoptosis (6).

Until now, the agents applied in clinics have failed to successfully treat patients with AD. It has been reported that antioxidants can help maintain cellular redox homeostasis, which may have beneficial effects on AD (7). Natural products constitute a large and underappreciated source of candidate agents for AD treatment (8,9). By modulating mitochondria-mediated apoptotic signaling, *Sparassis crispa* polysaccharide has been demonstrated to successfully protect PC12 cells against L-glutamic acid (L-Glu) damage (10). In an AlCl$_3$- and D-galactose (D-gal)-induced AD mouse model, which exhibits AD-like behaviors, *Hericium erinaceus* alleviated AD-like symptoms via the modulation of neurotransmitter levels and apoptosis associated with mitochondrial function (11). Scutellarin (SC), mainly extracted from the Chinese herb *Erigeron breviscapus* (vant.), has been reported to possess various pharmacological

Correspondence to: Dr Ling Kou, Department of Cardiology, Affiliated Hospital of Jiangsu University, Jiangsu University, 438 Jiefang Road, Zhenjiang, Jiangsu 212001, P.R. China
E-mail: kouling@ujs.edu.cn

Dr Xiaofeng Wang, Department of Stomatology, China-Japan Union Hospital of Jilin University, Jilin University, 126 Xiantai Street, Changchun, Jilin 130033, P.R. China
E-mail: xiaofeng2238@sina.com

benefits, particularly for neurological disorders (12). SC can attenuate neuronal injury by restoring the imbalance of excitatory vs. inhibitory amino acids and reducing oxidative stress (12). In addition, SC has been demonstrated to protect rats against ischemic injury mainly via the downregulation of endogenous metabolite levels (13).

Based on previous research, the present study aimed to investigate the protective effects of SC against L-Glu-induced HT22 cell damage, and AlCl₃- and D-gal-induced AD-like behavior. The results indicated that SC enhanced cell viability, reduced cell apoptosis, restored mitochondrial function, and regulated anti- and pro-apoptotic protein expression in L-Glu-induced HT22 cells. In the AD mouse model in the present study, SC successfully improved behavior, physiological and biochemical indices. The data suggested that SC may be used as an adjuvant therapy in AD and exerts its effects via the regulation of oxidative stress-induced mitochondrial-mediated apoptosis.

Materials and methods

Cell culture. The mouse hippocampal neuronal HT22 cell line (cat. no. BNCC-337709; Cell Bank of Type Culture Collection of the Chinese Academy of Sciences, Shanghai, China), was cultured in Dulbecco's modified Eagle's medium (DMEM; Invitrogen; Thermo Fisher Scientific, Inc., Waltham, MA, USA) supplemented with 10% fetal bovine serum (Invitrogen; Thermo Fisher Scientific, Inc.), 100 U/ml penicillin and 100 μg/ml streptomycin (Invitrogen; Thermo Fisher Scientific, Inc.) in a humidified atmosphere containing 5% CO_2 at 37˚C.

Cell viability, lactate dehydrogenase (LDH) release and caspase-3 activity analysis. HT22 cells were seeded into 96-well plates (6,000 cells/100 μl/well), pre-treated with 5 and 15 μM SC (CAS no. 27740-01-8; Shanghai YuanYe Biotechnology Co. Ltd., Shanghai, China), respectively for 3 h, and then exposed to 25 mM L-Glu (Sigma-Aldrich; Merck KGaA, Darmstadt, Germany) for a further 24 h at 37˚C. The cell culture medium was collected to measure the release of LDH using an *in vitro* Toxicology Assay kit [Cytotoxicity Detection Kit (LDH); Sigma-Aldrich; Merck KGaA], according to a previous study (14). A MTT assay (Sigma-Aldrich; Merck KGaA) was used to detect cell viability as previously described (15).

A total of 5x10⁵ HT22 cells were seeded into 6-well plates, pre-treated with 5 and 15 μM SC for 3 h, and then exposed to 25 mM L-Glu for a further 24 h as aforementioned. Caspase-3 activity was analyzed using a Caspase-3 activity assay kit (cat. no. G015; Nanjing Jiancheng Bioengineering Institute, Nanjing, China).

Cell apoptosis assay. A total of 5x10⁵ of HT22 cells were seeded into 6-well plates, pre-treated with 5 and 15 μM SC for 3 h, and then exposed to 25 mM L-Glu for a further 24 h as aforementioned. Cells were collected and stained using a Dead Cell Kit (propidium iodide and Annexin V; cat. no. MCH100105; EMD Millipore, Billerica, MA, USA) for 15 min at 25˚C in the dark. The Muse® Cell Analyzer from EMD Millipore was used to analyze cell fluorescence.

Assessment of intracellular ROS levels and dissipation of mitochondrial membrane potential (MMP). A total of 5x10⁵ HT22 cells were seeded into 6-well plates, pre-treated with 5 and 15 μM SC for 3 h, and then exposed to 25 mM L-Glu for a further 12 h, which was determined according to the results of preliminary experiments. Treated cells were stained with 5 μM 2,7-dichlorofluorescein diacetate (Sigma-Aldrich; Merck KGaA) for 20 min at room temperature in the dark, and the intracellular ROS levels were observed using a fluorescence microscope (magnification, x200; Axio Observer Z1; Carl Zeiss AG, Oberkochen, Germany). Quantitative data analysis was performed using ImageJ software version 1.46 (National Institutes of Health, Bethesda, MD, USA) and data were expressed as the green fluorescence intensity.

The treated cells were also stained with 2 μM JC-1 (Sigma-Aldrich; Merck KGaA) for 15 min at room temperature in the dark. Alterations in fluorescence were detected using a fluorescence microscope (magnification, x200; Axio Observer Z1; Carl Zeiss AG). The data were analyzed with ImageJ software and expressed as the ratio of red to green fluorescence intensity.

Western blot analysis. A total of 5x10⁵ HT22 cells were seeded into 6-well plates, pre-treated with 5 and 15 μM SC for 3 h, and then exposed to 25 mM L-Glu for a further 24 h as aforementioned. Treated cells were lysed with radioimmunoprecipitation assay buffer (Sigma-Aldrich; Merck KGaA) containing 1% protease inhibitor cocktail (Sigma-Aldrich; Merck KGaA). Following the determination of protein concentration using a bicinchoninic acid assay protein kit (EMD Millipore), 40 μg protein was loaded onto the gel and separated by 12% SDS-PAGE. The separated proteins were electrophoretically transferred onto 0.45 μm nitrocellulose membranes (Bio Basic, Inc., Markham, ON, Canada). The membranes were then blocked using 5% bovine serum albumin (Beijing Dingguo Changsheng Biotechnology Co., Ltd., Beijing, China) at 4˚C for 4 h. The membranes were incubated with primary antibodies at a dilution of 1:2,000 for 12 h at 4˚C: Cleaved caspase-3 (cat. no. 9661), B-cell lymphoma 2 (Bcl-2; cat. no. 3498), B-cell lymphoma-extra large (Bcl-xL; cat. no. 2764), Bcl-2-associated X protein (Bax; cat. no. 14796) and GAPDH (cat. no. 5174), and were all Santa Cruz Biotechnology, Inc., Dallas, TX, USA). Following three washes with Tris-buffered saline containing 0.1% Tween-20, the membranes were incubated with horseradish peroxidase-conjugated anti-rabbit IgG secondary antibodies (cat. no. 7074; Santa Cruz Biotechnology, Inc.) at a dilution of 1:3,000 for 3 h at 25˚C. Enhanced chemiluminescence kit (GE Healthcare Life Sciences, Little Chalfont, UK) was used to visualize the bands and ImageJ software was used to quantify the band intensity. Assays were performed in triplicate.

AD mouse model and treatment. The Institution Animal Ethics Committee of Jilin University approved the experimental protocol (approval no. 20170012) conducted in the present study. A total of 42 Balb/c male mice (10-weeks-old, 20-24 g) were purchased from the Norman Bethune University of Medical Science, Jilin University (Changchun, China) and housed in cages in a temperature-controlled room at 23±1˚C

with 40-60% humidity and a 12/12 h light/dark cycle, as well as sufficient access to water and food.

Of the 42 mice, 30 were subcutaneously injected 120 mg/kg D-gal and orally treated with 20 mg/kg AlCl₃ once per day for 8 weeks to establish an AD mice model similar to a previous study (16). At the fifth week, only 24 mice were retained for further experimentation, as the remaining 6 mice failed to exhibit AD-associated behaviors in the water maze test, and these 24 mince were then randomly divided into two groups, which were either treated orally with normal saline solution (n=12) or 20 mg/kg of SC (n=12) for 4 weeks. Normal mice (n=12) treated orally with normal saline solution for 8 weeks, served as the control group. From week 9, behavioral tests, including autonomic activity and a Morris water maze tests, were performed according to a previous study without modifications (16). Orbital blood (300 μl) was sampled via peritoneal injection following anesthesia with 400 mg/kg of 10% chloral hydrate. Following euthanasia by injection with 150 mg/kg 1.5% pentobarbital, whole brain tissues were collected.

Determination of acetylcholine (Ach), choline acetyltransferase (ChAT), superoxide dismutase (SOD), ROS and Aβ1-42 levels in the brain and/or serum. The levels of Ach [cat. nos. A105-1 (for brain tissues) and A105-2 (for serum); Nanjing Jiancheng Bioengineering Institute, Nangjing, China], ChAT [cat. nos. A079-1 (for brain tissues) and A079-2 (for serum); Nanjing Jiancheng Bioengineering Institute], Aβ1-42 (cat. no. E-20118; Shanghai Yuanye Biological Technology Co., Ltd., Shanghai, China) and SOD (cat. no. A001-3; Shanghai Yuanye Biological Technology Co., Ltd.) in the serum and brain tissues, as well as ROS (cat. no. E-20634; Shanghai Yuanye Biological Technology Co., Ltd., Shanghai, China) in brain tissues alone, were measured using ELISA kits.

Immunohistochemistry. Following collection, the brain tissues were fixed in 10% neutral formalin at room temperature for 48 h, and were then desiccated and embedded in paraffin (7 μm thick). The sections were then soaked in a descending alcohol series and then washed with deionized water and PBS for 5 min each. Following this, the paraffin sections were soaked in 0.01 M boiled citrate buffer at 95°C for 20 min in order to perform antigen retrieval. The protein expression levels of Aβ1-42 and phosphorylated (p)-Tau in brain tissue were detected via immunohistochemical analysis. Briefly, the slides of brain samples were heated in citrate buffer for 15 min to retrieve antigens, incubated with 3% hydrogen peroxide for 10 min at room temperature to block endogenous peroxidase and by blocked with 2% goat serum (Histostain™-Plus Kits; cat. no. SP-0023; Nanjing Jiancheng Bioengineering Institute) dissolved in PBS (16). The slides were the incubated with antibodies against Aβ1-42 (1:200; cat. no. bs-0877R; Beijing Biosynthesis Biotechnology Co., Ltd., Beijing, China) and p-Tau (1:200; cat. no. bs-2392R; Beijing Biosynthesis Biotechnology Co., Ltd.) for 12 h at 4°C. After washing with PBS, the slides were incubated with a horseradish peroxidase-conjugated secondary antibody (1:2,000; cat. no. sc-7074; Santa Cruz Biotechnology, Dallas, TX, USA) at 25°C for 4 h. The slides were visualized with 3,3'-diaminobenzidine for 3 min at room temperature and Mayer's hematoxylin for 3 min at room temperature, and were dehydrated with ethanol and xylene.

Finally, images were captured using an Olympus IX73 light microscope (magnification, x100; Olympus, Tokyo, Japan). The intensity of Aβ1-42 and p-Tau expression was analyzed using ImageJ software.

Statistical analysis. All experimental data are presented as the mean ± standard deviation. Statistical data were analyzed using one-way analysis of variance followed by a Duncan's multiple range post hoc test. Statistical analysis was conducted using SPSS v.16.0 software (SPSS, Inc., Chicago, IL, USA). P<0.05 was considered to indicate a statistically significant difference.

Results

SC protects HT22 cells against L-Glu-induced damage. Normal HT22 cells treated with SC (Fig. 1A) alone exhibited no significant alterations in cell viability compared with in the control; however, a significant decrease in cell viability was observed in response to L-Glu (P<0.01; Fig. 1B). Treating L-Glu-damaged cells with SC improved cell viability by >12% (P<0.05; Fig. 1B). Pre-treatment with 15 μM SC significantly reduced LDH release by 43.9% (P<0.01; Fig. 1C) and caspase-3 activity by 98.7% (P<0.001; Fig. 1D) compared with L-Glu-treated HT22 cells. In addition, HT22 cells exposed to 25 mM L-Glu exhibited an apoptosis rate of 18.1% (Fig. 1E). The cell apoptosis was reduced to 9.4% in cells pre-treated with 15 μM SC (Fig. 1E).

SC reduces ROS accumulation, restores MMP dissipation, and regulates anti- and pro-apoptotic protein expression. In L-Glu-treated HT22 cells, levels of intracellular ROS accumulation were indicated by enhanced green fluorescence; significant ROS accumulation was observed in response to L-Glu treatment compared with in the control (Fig. 2A). Dissipation of MMP was also observed, as indicated by a change of red to green fluorescence (Fig. 2B). Pre-treatment with 5 and 15 μM SC significantly suppressed the accumulation of ROS (P<0.001; Fig. 2A) and restored MMP dissipation compared with in the L-Glu-treated HT22 cells (P<0.001; Fig. 2B).

L-Glu-damaged cells revealed low protein expression levels of Bcl-2 and Bcl-xL, but high protein expression levels of Bax and cleaved caspase-3 compared with in control HT22 cells (P<0.01; Fig. 2C). Pre-incubation with SC resulted in >35.1 and 33.8% increase in Bcl-2 and Bcl-xL expression levels, respectively (P<0.01; Fig. 2C). Conversely, Bax (P<0.01) and cleaved caspase-3 (P<0.05; Fig. 2C) expression levels were reduced by >48.7 and 33.6%, respectively. These results suggested that SC protected HT22 cells against L-Glu-induced apoptosis via regulation of mitochondrial function.

SC alleviates behavioral symptoms in AD mice. Behavioral testing was performed in a D-gal plus AlCl₃ mouse model of AD to investigate the therapeutic effects of SC on AD. Compared with non-treated AD mice, SC significantly enhanced the number of vertical movements by 44.6% (P<0.01; Fig. 3A) and horizontal movements by 35.2% (P<0.01; Fig. 3B) in an autonomic activity test.

The water maze test can be applied to evaluate the learning and memory abilities of animals, and is commonly
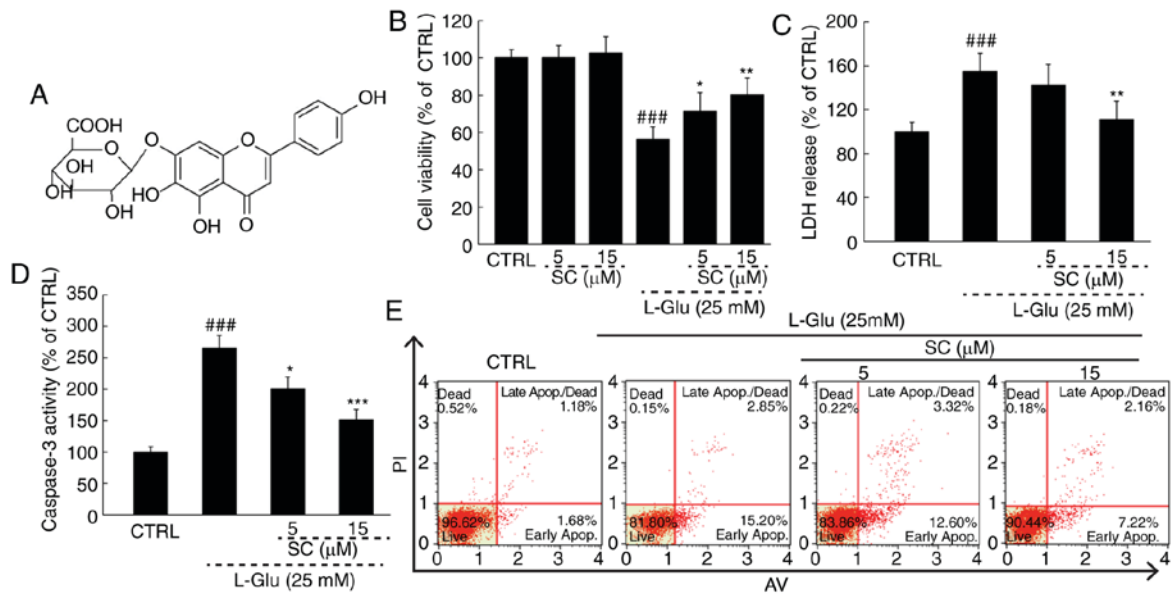
Figure 1. SC protects HT22 cells against L-Glu-induced damage. (A) Chemical structure of SC. HT22 cells were pre-incubated with 5 and 15 μM SC for 3 h, and then exposed to L-Glu for another 24 h. (B) SC enhanced cell viability as measured by MTT assay. (C) SC suppressed LDH release as measured using an *In vitro* Toxicology Assay kit. (D) SC decreased caspase-3 activation. (E) Flow cytometric analysis revealed that SC reduced apoptosis. Data are expressed the as the mean ± standard deviation (n=6). ###$P<0.001$ vs. CTRL; *$P<0.05$, **$P<0.01$, ***$P<0.001$ vs. L-Glu. AV, Annexin V; CTRL, control; LDH, lactate dehydrogenase; L-Glu, L-glutamic acid; PI, propidium iodide; SC, scutellarin.
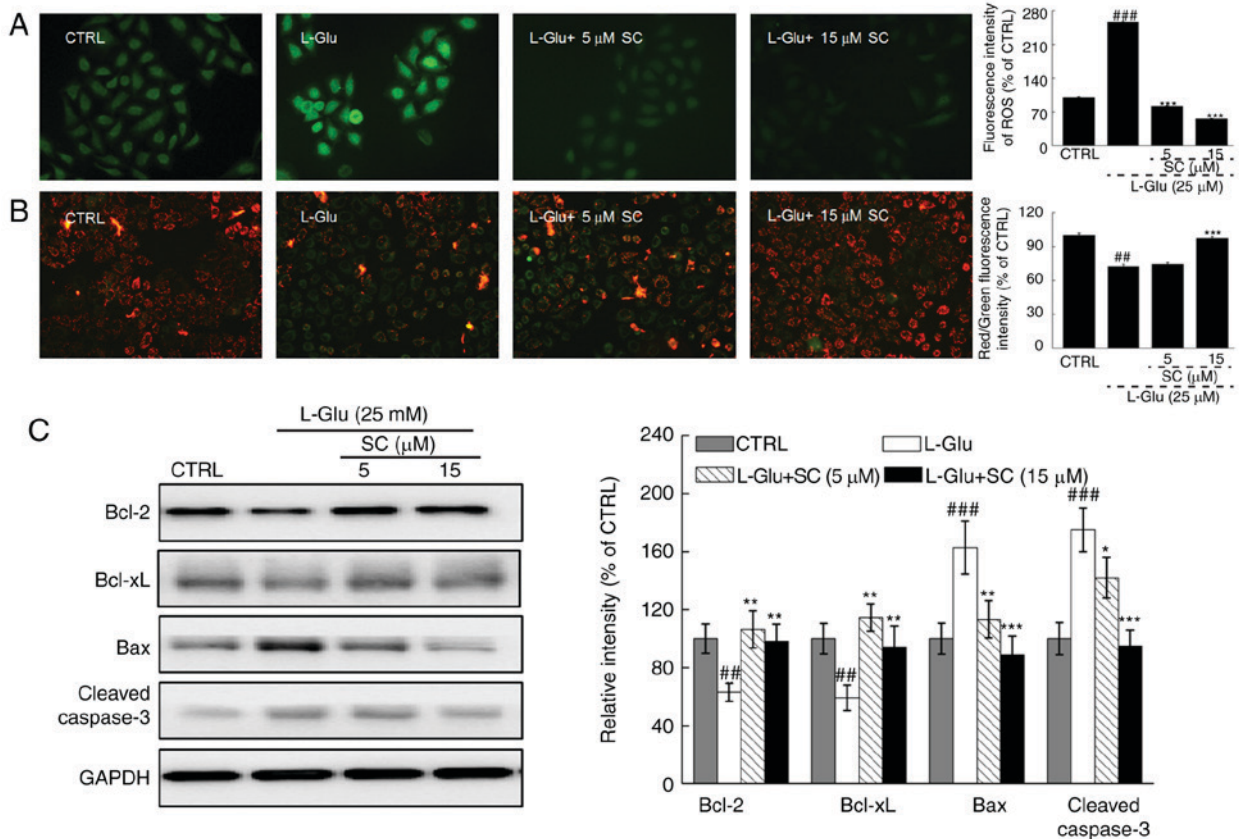

Figure 2. SC reduces ROS accumulation, restores MMP dissipation, and regulates anti- and pro-apoptotic protein expression. HT22 cells were pre-incubated with 5 and 15 μM SC for 3 h, and exposed to L-Glu for another 12 h. (A) Representative immunofluorescent images of HT22 stained with 2,7-dichloro-fluorescein diacetate to visualize intracellular ROS (magnification, x200; n=6). SC suppressed the accumulation of ROS, as demonstrated by reductions in green fluorescence intensity. (B) Immunofluorescence staining with JC-1 revealed that SC restored the dissipation of MMP (magnification, x200; n=6). The quantitative data of the ratio of red to green fluorescence intensity is presented on the right. (C) Following treatment with SC, cells were treated with L-Glu for another 24 h. Western blot analysis demonstrated that 15 μM SC was able to restore the expression of anti-apoptotic (Bcl-2 and Bcl-xL) and pro-apoptotic (Bax and cleaved caspase-3) proteins to normal levels. Quantification data were normalized to GAPDH and expressed as a percentage of CTRL (n=3). ##$P<0.01$, ###$P<0.001$ vs. CTRL; *$P<0.05$, **$P<0.01$, ***$P<0.001$ vs. L-Glu. Bax, Bcl-2-associated X protein; Bcl-2, B-cell lymphoma 2; Bcl-xL, B-cell lymphoma-extra large; CTRL, control; L-Glu, L-glutamic acid; MMP, mitochondrial membrane potential; ROS, reactive oxygen species; SC, scutellarin.
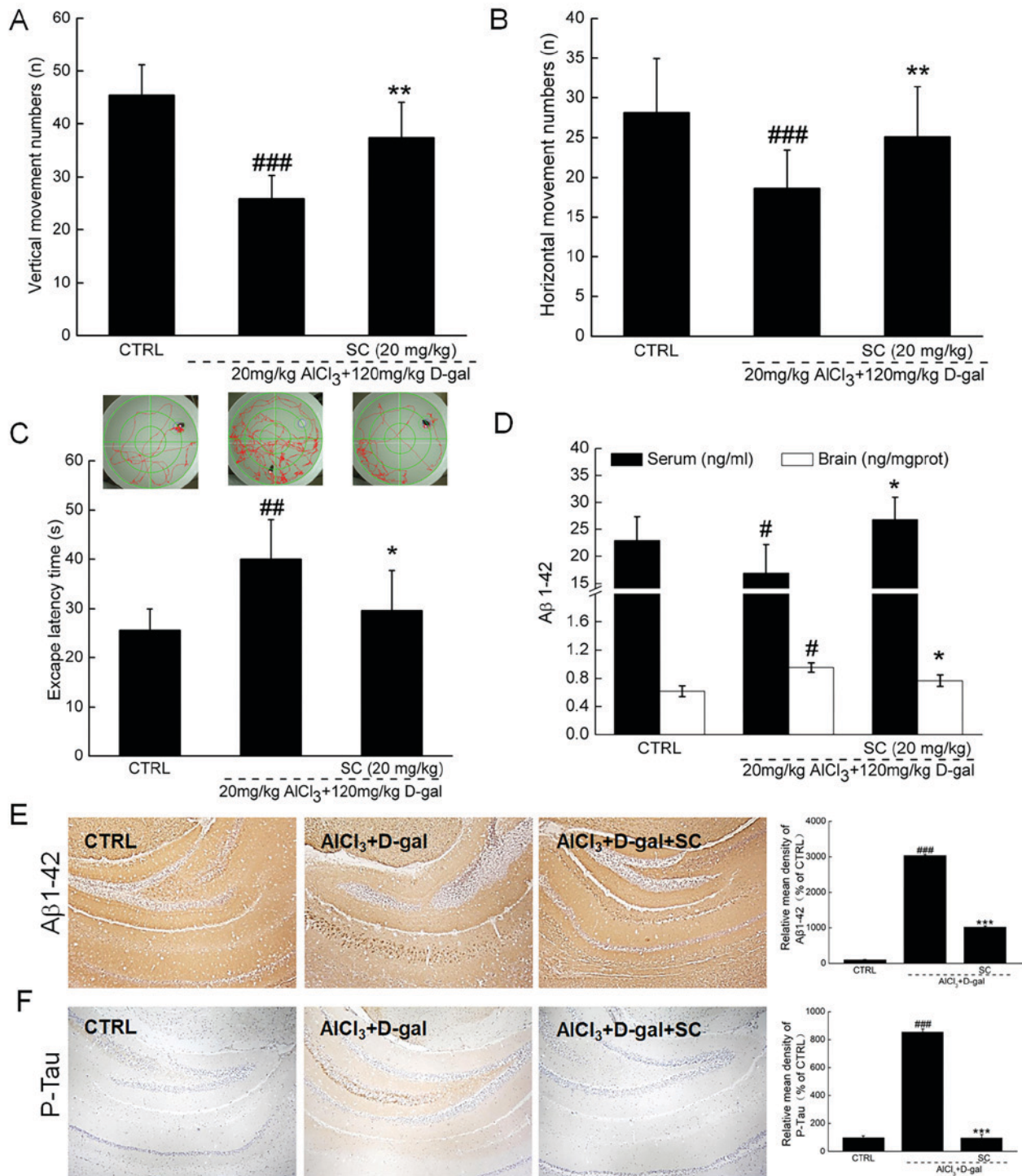
Figure 3. SC alleviates the clinical features of AD *in vivo*. In an AlCl$_3$ plus D-gal-induced mouse model of AD, 4-week SC administration enhanced (A) vertical and (B) horizontal movements in an autonomous activity test (n=12). (C) SC treatment decreased the escape latency time in a water maze test (n=12). (D) SC enhanced the serum levels of Aβ1-42, but reduced the levels of Aβ1-42 in brain lysate as determined via ELISA (n=12). Immunohistochemistry revealed that SC reduced (E) Aβ1-42 and (F) p-Tau expression levels in the hippocampus (n=6). The quantitative data were expressed as percentage protein density of CTRL. Data are expressed as the mean ± standard deviation. #P<0.05, ##P<0.01, ###P<0.001 vs. CTRL; *P<0.05, **P<0.01 and ***P<0.001 vs. AlCl$_3$ plus D-gal. Aβ1-42, amyloid β1-42; AD, Alzheimer's disease; AlCl$_3$, aluminum chloride; CTRL, control; D-gal, D-galactose; p-Tau, phosphorylated-Tau; SC, scutellarin.

performed in AD research (17). Compared with in heathy mice, the escape latency time was significantly increased by 56.8% in AD mice (P<0.01; Fig. 3C). Administration of SC for 4 weeks led to a 26.3% reduction in escape latency time compared with in AD mice (P<0.05; Fig. 3C). The attenuation of AD-associated symptoms following treatment with

SC further suggested that SC exhibits therapeutic effects in AD in mice models.

SC regulates Aβ1-42 expression levels and p-Tau aggregation. Aβ1-42, which has strong aggregating properties, has been reported to be the key component of amyloid plaques (16).
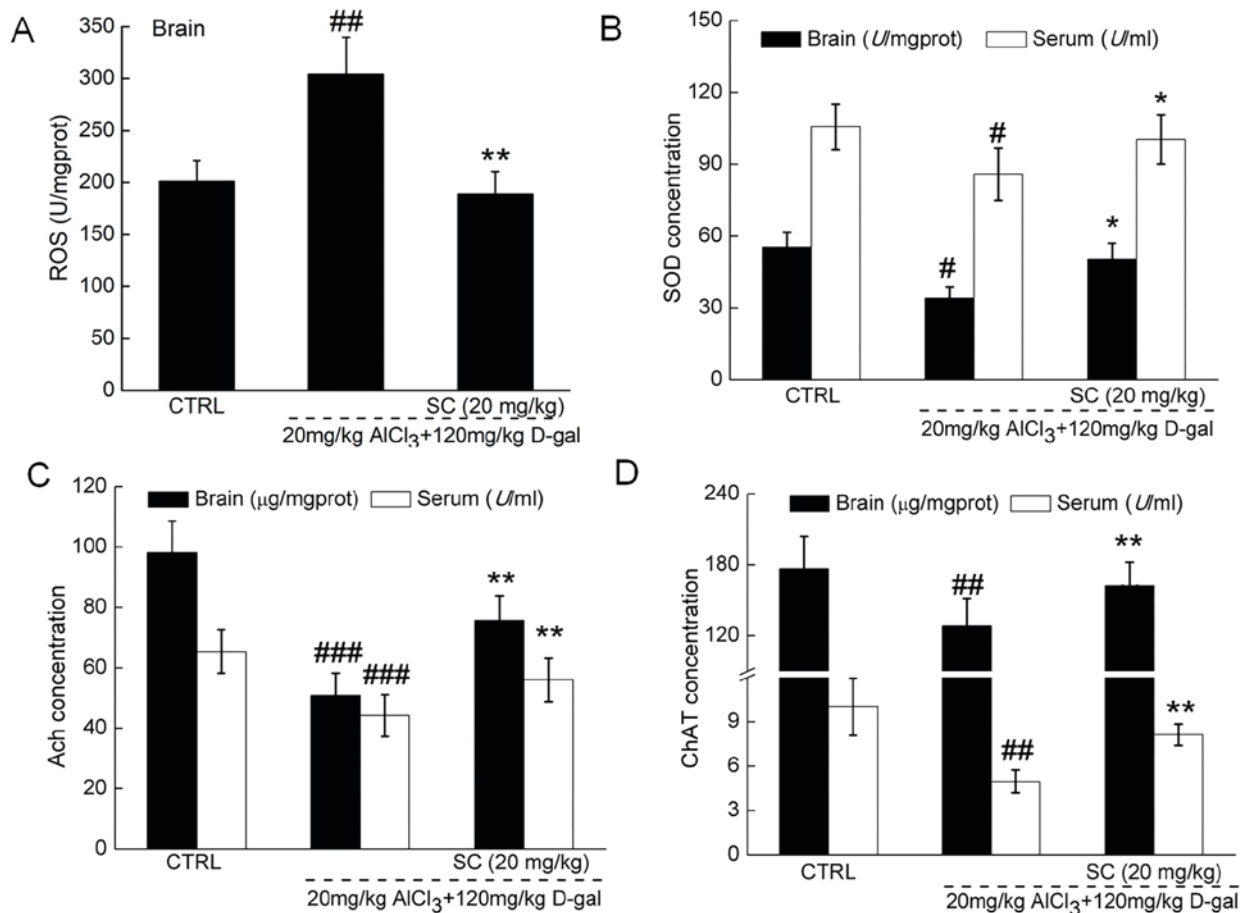
Figure 4. SC regulates ROS, SOD, Ach and ChAT *in vivo*. In an AlCl$_3$ plus D-gal-induced Alzheimer's disease mouse model, 4-week SC administration (A) reduced ROS levels in brain lysate, and enhanced the levels of (B) SOD, (C) Ach and (D) ChAT in the serum and brain lysate, as measured by ELISA. Data are expressed as the mean ± standard deviation (n=12). $^{\#}P<0.05$, $^{\#\#}P<0.01$, $^{\#\#\#}P<0.001$ vs. CTRL; $^{*}P<0.05$, $^{**}P<0.01$ vs. AlCl$_3$ plus D-gal. Aβ1-42, amyloid β1-42; Ach, acetylcholine; AlCl$_3$, aluminum chloride; ChAT, choline acetyltransferase; CTRL, control; D-gal, D-galactose; ROS, reactive oxygen species; SC, scutellarin; SOD, superoxide dismutase.

Following 4-week SC administration, the serum Aβ1-42 concentrations were increased by 48.1% compared with non-treated AD mice (P<0.05; Fig. 3D), whereas Aβ1-42 concentrations in brain were reduced by 19.6% (P<0.05; Fig. 3D). The results of immunohistochemical analysis indicated that, compared with in the nontreated SD group, SC significantly reduced the Aβ1-42 levels in brain, particularly in the region of the hippocampus (P<0.001; Fig. 3E).

Compared with control mice, the expression levels of p-Tau were significantly enhanced in the hippocampus of AD mice; however, SC administration significantly reduced the levels of p-Tau (P<0.001; Fig. 3F). The attenuation of effects associated with AD following treatment with SC may be due to resultant decreased levels of Aβ1-42 and p-Tau.

SC regulates Ach, ChAT, SOD and ROS. Compared with in control mice, the levels of SOD, Ach and ChAT in the serum and brain lysate samples were significantly lower in AD mice (P<0.05), whereas significantly increased levels of ROS were detected in the brain lysates of AD mice (P<0.01; Fig. 4A-D). For factors associated with oxidative stress, SC treatment significantly enhanced the concentration of SOD in the serum and brain lysate (P<0.05; Fig. 4B), and reduced the levels of ROS in the brain lysate of AD mice (P<0.01; Fig. 4A) compared

with in non-treated AD mice. In terms of cholinergic function, SC significantly increased the levels of Ach (P<0.01; Fig. 4C) and ChAT (P<0.01; Fig. 4D) in the serum and brains of AD mice compared with in the non-treated AD groups. The results suggested that regulation of oxidative stress and cholinergic function are associated with protective effects exhibited by SC against AD.

Discussion

The present study revealed the protective effects of SC against L-Glu-induced HT22 cell damage, as demonstrated by the amelioration of mitochondrial-mediated apoptosis. SC restored the MMP dissipation and suppressed the accumulation of intracellular ROS in L-Glu-damaged HT22 cells. Glutamate inhibits cysteine uptake, leading to necrosis and apoptosis due to the disequilibrium between oxidation and antioxidation, which affects ROS levels (18). High levels of ROS helps open mitochondrial permeability transition pores, resulting in the dissipation of MMP (19). A short feedback loop has been proposed between ROS levels and mitochondrial function, whereby enhanced cytoplasm ROS levels may lead to the dissipation of MMP and subsequent release of mitochondrial ROS as well as other pro-apoptotic

molecules, such as caspase-3, from the mitochondria to the cytoplasm (20). In addition, SC enhanced the expression levels of Bcl-2 and Bcl-xL, and reduced the levels of Bax in L-Glu-treated HT22 cells. Bcl-2 family members are present in the membrane of mitochondria and directly influence mitochondrial function by regulating the opening of mitochondrial permeability transition pores (21). These findings suggested that SC-mediated neuroprotection against L-Glu-induced neurotoxicity in HT22 cells may be associated with oxidative stress-induced mitochondrial-mediated apoptosis.

In AD mice, long-term D-gal injections cause ROS accumulation and mitochondrial dysfunction (22). Polyunsaturated fatty acids in the brain can be easily damaged by oxidative stress (23), which in turn affects learning and memory abilities (24). In addition, aluminum can form a complex with Aβ that can more readily access the brain and is responsible for cerebrovascular dysregulation (25). Aβ aggregation in the brain, serving as a hallmark of spatial memory deficit and cognitive dysfunction, can also cause imbalance to the oxidative stress system by inducing the overproduction of ROS during the progression of AD (26). However, the clearance of Aβ aggregation in the brains of patients with AD can increase Aβ levels in peripheral blood (27). The aggregation of Aβ may also further initiate the Tau pathology, contributing to the formation of neurofibrillary tangles (16). In the present study, mice with AD induced by AlCl$_3$ and D-gal revealed that SC enhanced the levels of SOD in the serum and brain lysate, reduced the levels of ROS in brain lysate, increased the concentration of Aβ1-42 in the serum, and suppressed Aβ1-42 aggregation and Tau protein deposition in the hippocampus area. SOD, an endogenous antioxidant, has been reported as the first-line of defense against oxidative damage (28). Combined with the *in vitro* results, SC-induced improvement in the cognitive performance of AD mice may be, at least partially, associated with its modulation of the balance of oxidative stress, which suppressed cell apoptosis.

In the present study, it was also revealed that SC significantly enhanced the levels of Ach and ChAT in the serum and brain lysate of AD mice. Impaired cholinergic function has been noted in patients with AD, and in particular, low levels of Ach and ChAT have been reported to contribute to cognitive and memory decline (29). Ach, dynamically controlled by AchE, is responsible for the storage and recovery of long-term memory (28). Previous studies demonstrated that *Armillaria mellea* and *Amanita caesarea* can improve AD-like behaviors via enhancing the levels of Ach and ChAT in the serum and brains of AlCl$_3$- and D-gal induced AD mice (15,17). The data in the present study suggested that SC-mediated protection against AD may be associated with its regulation of cholinergic function. However, the association between cholinergic transmitters and oxidative stress remains unknown and further investigation is required.

In conclusion, SC exhibited neuroprotective effects against L-Glu-induced neurotoxicity in HT22 cells and alleviated AD-like behaviors in mice, which may largely be attributable to its antioxidation and antiapoptotic properties. These findings support SC as a potential agent for the prevention and/or adjuvant therapy for AD.

Availability of data and materials

All data generated and analyzed during the present study are included in this published article.

Authors' contributions

XW and LK designed the experiments; XH, ST, JH, MD and XS performed the experiments and processed data; XH, XW and LK wrote the manuscript; MD, XW and LK revised the manuscript.

Ethics approval and consent to participate

Institution Animal Ethics Committee of Jilin University approved the experimental protocol (approval no. 20170012).

Patient consent for publication

Not applicable.

Competing interests

The authors declare that they have no competing interests.

References

1. Rygiel K: Novel strategies for Alzheimer's disease treatment: An overview of anti-amyloid beta monoclonal antibodies. Indian J Pharmacol 48: 629-636, 2016.
2. Xu T, Niu C, Zhang X and Dong M: β-Ecdysterone protects SH-SY5Y cells against β-amyloid-induced apoptosis via c-Jun N-terminal kinase- and Akt-associated complementary pathways. Lab Invest 98: 489-499, 2018.
3. Rosello A, Warnes G and Meier UC: Cell death pathways and autophagy in the central nervous system and its involvement in neurodegeneration, immunity and central nervous system infection: To die or not to die-that is the question. Clin Exp Immunol 168: 52-57, 2012.
4. Daulatzai MA: Cerebral hypoperfusion and glucose hypometabolism: Key pathophysiological modulators promote neurodegeneration, cognitive impairment and Alzheimer's disease. J Neurosci Res 95: 943-972, 2017.
5. Luo P, Fei F, Zhang L, Qu Y and Fei Z: The role of glutamate receptors in traumatic brain injury: Implications for postsynaptic density in pathophysiology. Brain Res Bull 85: 313-320, 2011.
6. Hu JF, Chu SF, Ning N, Yuan YH, Xue W, Chen NH and Zhang JT: Protective effect of (-)clausenamide against Abeta-induced neurotoxicity in differentiated PC12 cells. Neurosci Lett 483: 78-82, 2010.

7. Zhao Y and Zhao B: Natural antioxidants in prevention and management of Alzheimer's disease. Front Biosci (Elite Ed) 4: 794-808, 2012.
8. Wang D, Tan QR and Zhang ZJ: Neuroprotective effects of paeoniflorin, but not the isomer albiflorin, are associated with the suppression of intracellular calcium and calcium/calmodulin protein kinase II in PC12 cells. J Mol Neurosci 51: 581-590, 2013.
9. Wang D, Guo TQ, Wang ZY, Lu JH, Liu DP, Meng QF, Xie J, Zhang XL, Liu Y and Teng LS: ERKs and mitochondria-related pathways are essential for glycyrrhizic acid-mediated neuroprotection against glutamate-induced toxicity in differentiated PC12 cells. Braz J Med Biol Res 47: 773-779, 2014.
10. Hu S, Wang D, Zhang J, Du M, Cheng Y, Liu Y, Zhang N, Wang D and Wu Y: Mitochondria related pathway is essential for polysaccharides purified from sparassis crispa mediated neuro-protection against glutamate-induced toxicity in differentiated PC12 cells. Int J Mol Sci 17: pii: E133, 2016.
11. Zhang J, An S, Hu W, Teng M, Wang X, Qu Y, Liu Y, Yuan Y and Wang D: The Neuroprotective properties of hericium erinaceus in glutamate-damaged differentiated PC12 cells and an Alzheimer's disease mouse model. Int J Mol Sci 17: pii: E1810, 2016.
12. Tang H, Tang Y, Li N, Shi Q, Guo J, Shang E and Duan JA: Neuroprotective effects of scutellarin and scutellarein on repeatedly cerebral ischemia-reperfusion in rats. Pharmacol Biochem Behav 118: 51-59, 2014.
13. Tang H, Tang Y, Li NG, Lin H, Li W, Shi Q, Zhang W, Zhang P, Dong Z and Shen M: Comparative metabolomic analysis of the neuroprotective effects of scutellarin and scutellarein against ischemic insult. PLoS One 10: e0131569, 2015.
14. Wang D, Lu J, Liu Y, Meng Q, Xie J, Wang Z and Teng L: Liquiritigenin induces tumor cell death through mitogen-activated protein kinase-(MPAKs-) mediated pathway in hepatocellular carcinoma cells. BioMed Res Int 2014: 965316, 2014.
15. An S, Lu W, Zhang Y, Yuan Q and Wang D: Pharmacological basis for use of Armillaria mellea polysaccharides in Alzheimer's disease: Antiapoptosis and antioxidation. Oxid Med Cell Longev 2017: 4184562, 2017.
16. Zhao JM, Li L, Chen L, Shi Y, Li YW, Shang HX, Wu LY, Weng ZJ, Bao CH and Wu HG: Comparison of the analgesic effects between electro-acupuncture and moxibustion with visceral hypersensitivity rats in irritable bowel syndrome. World J Gastroenterol 23: 2928-2939, 2017.
17. Li Z, Chen X, Lu W, Zhang S, Guan X, Li Z and Wang D: Anti-oxidative stress activity is essential for Amanita caesarea mediated neuroprotection on glutamate-induced apoptotic HT22 cells and an Alzheimer's disease mouse model. Int J Mol Sci 18: pii: E1623, 2017.
18. Brown DI and Griendling KK: Regulation of signal transduction by reactive oxygen species in the cardiovascular system. Circ Res 116: 531-549, 2015.
19. Circu ML and Aw TY: Reactive oxygen species, cellular redox systems, and apoptosis. Free Radic Biol Med 48: 749-762, 2010.
20. Lemasters JJ, Qian T, Trost LC, Herman B, Cascio WE, Bradham CA, Brenner DA and Nieminen AL: Confocal microscopy of the mitochondrial permeability transition in necrotic and apoptotic cell death. Biochem Soc Symp 66: 205-222, 1999.
21. Gross A and Katz SG: Non-apoptotic functions of BCL-2 family proteins. Cell Death Differ 24: 1348-1358, 2017.
22. Qu Z, Zhang J, Yang H, Huo L, Gao J, Chen H and Gao W: Protective effect of tetrahydropalmatine against d-galactose induced memory impairment in rat. Physiol Behav 154: 114-125, 2016.
23. Jiang T, Sun Q and Chen S: Oxidative stress: A major pathogenesis and potential therapeutic target of antioxidative agents in Parkinson's disease and Alzheimer's disease. Prog Neurobiol 147: 1-19, 2016.
24. Nemeth M, Millesi E, Wagner KH and Wallner B: Sex-specific effects of diets high in unsaturated fatty acids on spatial learning and memory in guinea pigs. PLoS One 10: e0140485, 2015.
25. Banks WA, Niehoff ML, Drago D and Zatta P: Aluminum complexing enhances amyloid beta protein penetration of blood-brain barrier. Brain Res 1116: 215-221, 2006.
26. Kim DI, Lee KH, Gabr AA, Choi GE, Kim JS, Ko SH and Han HJ: Abeta-induced Drp1 phosphorylation through Akt activation promotes excessive mitochondrial fission leading to neuronal apoptosis. Biochim Biophys Acta 1863: 2820-2834, 2016.
27. Fei M, Jianghua W, Rujuan M, Wei Z and Qian W: The relationship of plasma Aβ levels to dementia in aging individuals with mild cognitive impairment. J Neurol Sci 305: 92-96, 2011.
28. Islam MT: Oxidative stress and mitochondrial dysfunction-linked neurodegenerative disorders. Neurol Res 39: 73-82, 2017.
29. Farkas E and Luiten PG: Cerebral microvascular pathology in aging and Alzheimer's disease. Prog Neurobiol 64: 575-611, 2001.